Journal of Cleaner Production 528 (2025) 146733

Contents lists available at ScienceDirect

Journal of Cleaner Production

journal homepage: www.elsevier.com/locate/jclepro

Floating solar photovoltaic energy for coastal areas: A siting methodology

D.M. Fouz [a], R. Carballo [b,*], I. López [b], B. Álvarez [b], G. Iglesias [c,d]

[a] PROePLA (GI-1716), Área de Proyectos de Ingeniería, EPSE, Campus Terra, Univ. de Santiago de Compostela, 27002, Lugo, Spain
[b] Área de Ingeniería Hidráulica, EPSE, Campus Terra, Univ. de Santiago de Compostela, 27002, Lugo, Spain
[c] School of Engineering and Architecture & MaREI, Environmental Research Institute, University College Cork, College Road, P43 C573, Cork, Ireland
[d] School of Engineering, Computing and Mathematics, University of Plymouth, Marine Building, Drake Circus, PL4 8AA, Plymouth, UK

HIGHLIGHTS

- The novel Integrated Floating Solar Energy (IFSE) index is developed.
- A method for site selection of FPV systems in coastal areas is applied.
- The IFSE index is applied to the Ría de Vigo.
- Nearshore areas for FPV systems operation in the Ría de Vigo are identified.

ARTICLE INFO

Keywords:
Floating solar energy
FPV systems
Nearshore areas
Estuaries
CAPEX

ABSTRACT

The decision-making process at the early stages of marine renewable energy projects typically faces considerable uncertainties. Amongst them, identifying the most suitable cost-effective locations is a key aspect, for which several novel indices have been proposed recently. In the case of floating solar photovoltaic (FPV) energy, a nascent technology, efforts have focused on offshore sites, possibly to the detriment of nearshore options of high interest such as estuaries. Granted, coastal areas present specific challenges, not least their high environmental value and the coexistence of many uses of the marine space, the compatibility of which ought to be accurately assessed. In this work, the Integrated Floating Solar Energy (IFSE) index is proposed for siting FPV farms in coastal areas. This novel index is based on a comprehensive methodology, which considers the aspects relevant to the decision-making process: (i) the exploitable resource, (ii) the costs of installation, and (iii) the socioeconomic and environmental aspects. The IFSE index is applied to a case study in the Ría de Vigo, an estuary in NW Spain, leading to the delimitation of an area of about 7 km^2 as that with the highest interest, and showing the capability of this index to significantly contribute to the decision-making process for the deployment of FPV farms in coastal areas.

1. Introduction

The diversification and decarbonisation of the energy mix stand out as key efforts of the international community towards reaching climate neutrality objectives (Ghorbani et al., 2024). In this context, renewable energies, and especially solar and wind energy, have reached remarkable quotas of carbon-free energy production (Sarkodie et al., 2023); however, land scarcity constitutes a major difficulty for their further expansion in developed countries (Fang et al., 2024), with traditional renewables being subject to endless controversy between different stakeholders (e.g., energy vs. food production debate) (Turney and Fthenakis, 2011). As a result, marine and coastal environments have been postulated as potential areas for installing solar (Martínez and Iglesias, 2024a) and wind (Thomas et al., 2025) as well as wave (López, I. et al., 2024) and hydrokinetic (Carballo et al., 2024) energy farms.

In this context, floating solar photovoltaic (FPV) energy is undergoing an impressive growth, with an average increment per year in terms of installed power of approx. 130 % over the last decade (Rosa-Clot and Tina, 2020). Despite the novelty of the installation of FPV technology in marine and coastal areas, commercial FPV systems have already been effectively deployed in different freshwater bodies worldwide (Wei et al., 2025), revealing a significant number of promising locations in regions with high levels of insolation (e.g., Elminshawy et al., 2024). These facilities have shown promising advantages in

* Corresponding author.
E-mail address: rodrigo.carballo@usc.es (R. Carballo).

https://doi.org/10.1016/j.jclepro.2025.146733
Received 30 April 2025; Received in revised form 15 September 2025; Accepted 26 September 2025
Available online 1 October 2025

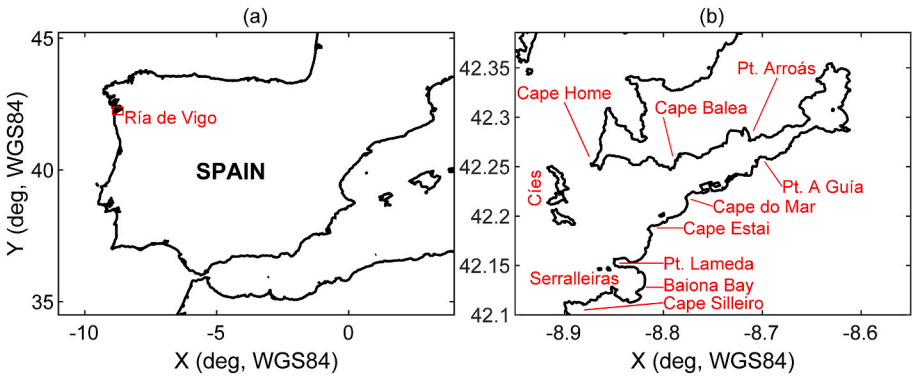

Fig. 1. Ría de Vigo (b) located in NW Spain (a).

comparison with ground-mounted PV (GPV) facilities, such as their higher efficiency, which is enhanced by the cooler marine and coastal environments, or the minimisation of shading losses resulting from the open nature of these areas (Claus and López, 2022). Nevertheless, in spite of their advantages, the levelized cost of energy (LCOE) of FPV technology (i.e., 0.05–0.10 €/kWh) is still higher than GPV systems (i.e., 0.03–0.05 €/kWh) (Oliveira-Pinto and Stokkermans, 2020). On these grounds, extensive research efforts are focused on reducing its LCOE figures through the development of new technology (e.g., López, M. et al., 2024) or the improvement in its installation (e.g., Claus and López, 2023), thus leading to optimize the performance of FPV systems (e.g., Elminshawy et al., 2024), along with their co-location with other renewable energy resources (Luhaniwal et al., 2024), especially wind energy (e.g., Huang and Iglesias, 2024).

Despite their value, these works are usually focused on the installation of FPV systems in offshore environments, disregarding their deployment in nearshore areas or semi-enclosed waterbodies, such as estuaries or bays, which have shown to be promising areas with lower LCOE (Martínez and Iglesias, 2024b). These types of waterbodies constitute complex coastal environments, usually characterised by an intricate geomorphology (i.e., shallow to intermediate water depths, including significant intertidal and emerged areas in their inner part, as well as narrow cross-sections), where an intense socioeconomic activity (e.g., aquaculture, shipping, etc.) coexists with several protected areas (e.g., Natura 2000), often in a limited available area. This results in abrupt spatial variations (i.e., over short distances) of the main constraints for the installation and operation of FPV systems, which strongly influence the resulting LCOE figures. In this regard, recent works have proposed a new FPV system adapted to estuarine areas (López, M. et al., 2024).

Therefore, the definition of reliable siting procedures for FPV technology in coastal areas is a key step towards its further development. Along with R&D activities focused on its technological development, these site-selection methods could constitute a starting point for the definition of more complex procedures (e.g., cost-effective analyses), specifically designed for the accurate computation of the LCOE of FPV systems in advanced-stage projects, as is the case of other marine renewable energy resources, such as wave (deCastro et al., 2024), hydrokinetic (Fouz et al., 2023) or offshore wind (Martínez and Iglesias, 2024c) energy, or offshore solar farms (Filgueira-Vizoso et al., 2025), and finally lead to the growth of the FPV sector with coastal deployments.

The main weakness of early-stage projects is the large number of uncertainties involved in their decision-making process. In order to reduce the uncertainties and facilitate the decision-making process, several novel indices have been recently proposed in the context of different marine renewable energy resources (e.g., Penalba et al., 2021), especially in the case of offshore wind energy (e.g., Bahaj et al., 2020), with particular emphasis on its co-location with wave energy farms (e.g., Majidi et al., 2025) and FPV systems (e.g., Frías-Paredes and Gastón--Romeo, 2025), including their long-term analysis (e.g., Ulazia et al., 2023).

Amongst the proposed indexes to analyse MRE projects, the IHE (Integrated Hydrokinetic Energy) index, originally developed for the site selection of hydrokinetic energy projects (Fouz et al., 2022), stands out for its ease of application to different coastal regions of interest, including nearshore areas such as estuaries or bays. The IHE index provides accurate and reliable results and thereby constitutes a first step towards conducting cost-effective analyses (Fouz et al., 2023). Overall, its application leads to the selection of the most appropriate area for energy exploitation in a coastal region, irrespective of the energy conversion technology and farm layout, by using a holistic approach integrating (Fouz et al., 2022): (i) the exploitable resource, (ii) the installation costs as a function of the coastal configuration, and (iii) the main socioeconomic and environmental constraints. This index was previously applied to identify the most appropriate areas for energy exploitation in tidally-driven estuaries, such as the Shannon Estuary (W Ireland) (Fouz et al., 2022), and subsequently adapted for its application to coastal areas whose hydrodynamics are dominated by large fluvial discharges, thereby subject to high seasonality, as is the case of the Miño Estuary (NW Iberian Peninsula) (Carballo et al., 2024).

In this work, and following a similar approach, a new index for siting FPV systems in estuarine areas, the IFSE (Integrated Floating Solar Energy) index, is developed by analysing not only the available energy resource, but also the exploitable resource, along with the installation costs, socioeconomic and environment aspects. The application of this new index is illustrated through a case study in the Ría de Vigo (NW Spain) (Fig. 1), a mesotidal coastal area with a surface area of 176 km^2, characterised by its sheltered conditions resulting from the natural barrier constituted by the Cíes Islands, whose favourable environmental conditions for FPV operation have been highlighted in previous works, focusing on its high irradiance levels throughout the year and moderate wave climate (López, M. et al., 2024).

The Ría de Vigo is the southernmost of the Galician Lower Rias (Rías Baixas), former tectonic valleys flooded during the Cenozoic era. It is geographically delimited between Capes Silleiro (42°06′44″N 8°53′57″W) and Home (42°15′10″N 8°52′12″W) to the north and south, respectively, being usually divided in three different parts: (i) the inner ria, to the east of Punta Arroás and Punta A Guía, (ii) the middle ria, to the west of the inner ria extending up to Cape Balea and do Mar, and (iii) the outer ria, to the west of the middle ria. According to the Köppen–Geiger–Pohl Climatic Classification (Peel et al., 2007), it presents a transitional climate between the warm-summer Mediterranean climate (Csb) and the oceanic climate (Cfb), tending more towards the first. As a result of its latitude (i.e., around 42°N), the Ría de Vigo presents average annual figures of global horizontal irradiance (GHI) of about 175–195 Wm^{-2} (López, M. et al., 2022), which corresponds to a relatively high resource availability (e.g., GHI ranges in Spain between

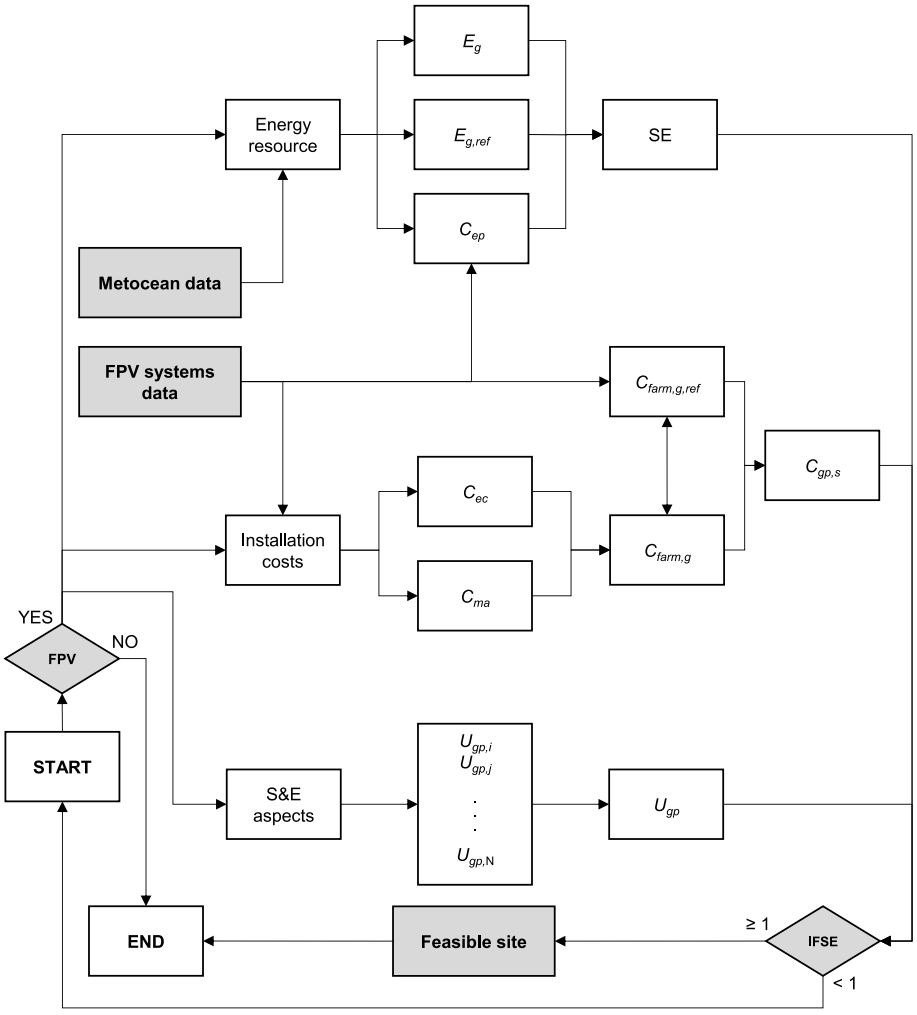

Fig. 2. Flowchart describing the whole method for applying the IFSE index.

147 and 235 Wm^{-2}), indicating its suitability for energy exploitation and therefore for FPV operation.

Previous works have analysed the suitability of the Ría de Vigo for FPV operation, and in particular for the installation of a new concept of FPV system, HelioSea, providing a first simplified estimate of LCOE figures resulting from its operation (López, M. et al., 2024), but without developing a detailed site selection. As a result, LCOE between 0.16 and 0.27 €/kWh have been preliminary estimated, i.e., around three times higher than typical offshore FPV operation with relatively higher commercial maturity. Thus, and despite the valuable interest of these initial approaches, the application, for the first time, of holistic site selection procedures to this coastal area, i.e., considering not only the energy resource but also other aspects such as the coastal configuration or the main socioeconomic and environmental restraints, could shed some light on the decision-making for FPV operation in the Ría de Vigo and, more generally, in nearshore coastal environments, providing key information as a preliminary step towards its accurate cost-effective analysis.

This article is organised as follows. First, in Section 2, a general overview of the IFSE index is presented. Then, in Sections 3 to 5, the different aspects and terms considered in the index are explained in detail. Next, in Section 6, the main results of the application of the IFSE index to the Ría de Vigo are presented and discussed in detail. Finally, in Section 7, the major conclusions and findings of the development of the index and its subsequent application are drawn.

2. General description of the method: an overview of the IFSE index

The IFSE index developed in this work aims to assess the location of FPV systems at early project stages. To this end, a similar approach to the so-called Integrated Hydrokinetic Energy (IHE) index is followed, being conceived as a holistic tool for identifying appropriate locations for hydrokinetic energy projects in coastal regions. This index considers all the relevant aspects involved in the decision-making process, namely (Fouz et al., 2022): (i) the exploitable energy resource, (ii) the main installation costs resulting from coastal configuration by applying a geospatial cost penalty function, C_{gp}, and (iii) socioeconomic and environmental (S&E) aspects through a geospatial water use penalty function, U_{gp}. The IHE index has shown to be a powerful tool, successfully applied for identifying the best sites for installing hydrokinetic energy farms in different coastal areas, including both shallow (Carballo et al., 2024) and deep areas (Fouz et al., 2022), constituting a first step towards their detailed cost-effective analysis (Fouz et al., 2023). However, the IHE index cannot be directly applied to other marine renewable energies, such as FPV.

Based on the IHE index, the Integrated Floating Solar Energy (IFSE) index is defined, being expressed as:

$$\mathrm{IFSE} = \mathrm{SE}\, C_{gp,s} U_{gp}\ , \tag{1}$$

where SE stands for the Solar Energy resource index, $C_{gp,s}$ is the geospatial cost penalty function adapted to solar energy exploitation and

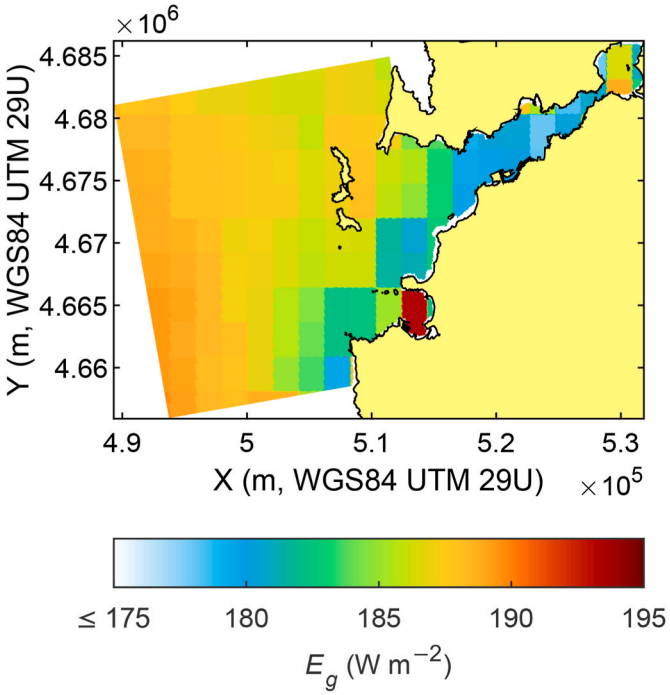

Fig. 3. Spatial distribution of E_g throughout the Ría de Vigo.

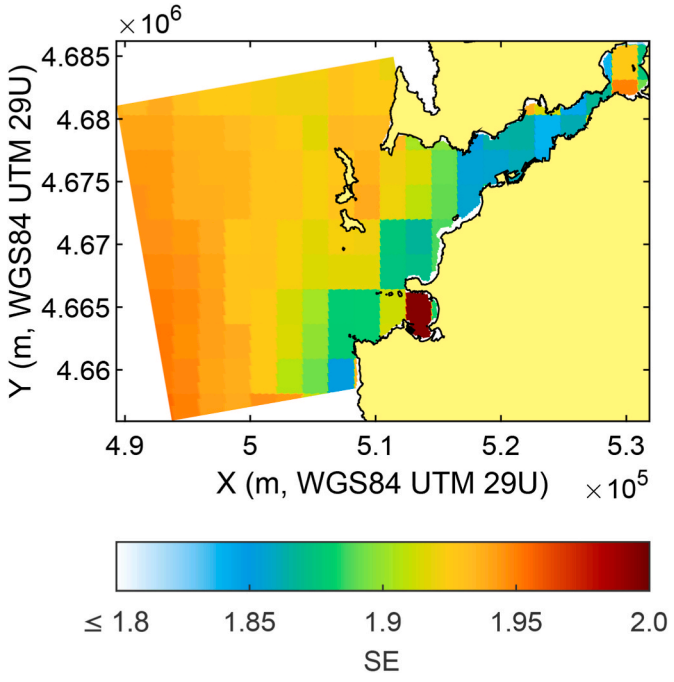

Fig. 4. Spatial distribution of the SE index throughout the Ría de Vigo.

U_{gp} represents the geospatial water use penalty function, accounting for the abovementioned aspects (i) to (iii), respectively, and applying the same physical interpretation as the IHE index, i.e., values of SE or IFSE $\geq$1 indicate suitability for installing FPV systems, with larger values indicating better locations, with $C_{gp,s}$ and U_{gp} functions ranging between 0 and 1.

In the following sections, the development of the parameters constituting the IFSE index and their application are explained in detail. In order to help the reader to understand the development and application of the IFSE index, a flowchart describing the whole procedure is provided in Fig. 2. Due to complexity in the definition of the procedure, the three involved functions are described in separate sections, namely: (i) the exploitable resource, SE (Section 3), (ii) the costs of installation, $C_{gp,s}$ (Section 4), and (ii) the socioeconomic and environmental aspects, U_{gp} (Section 5).

The IFSE index is conceived as a spatial planning tool which aims to address uncertainties throughout the decision-making processes at early FPV project stages. Therefore, it is necessary to highlight that final FPV farm designs would require detailed LCOE analysis of various technologies and array distribution combinations.

3. Solar energy (SE) resource index

3.1. Development of SE index

The first step towards the development of the IFSE index is to define the Solar Energy (SE) resource index as an indicator which should accurately characterise the suitability of coastal areas for solar energy exploitation from the point of view of the exploitability of the energy resource. With this aim, the SE index is defined as:

$$\mathrm{SE} = \frac{E_g}{E_{g,ref}} C_{ep}, \tag{2}$$

where E_g represents the yearly averaged value of the GHI over a horizontal surface considering both day and night-time (Fig. 3), $E_{g,ref}$ is a threshold value of E_g representing the minimum energy resource required for exploitation suitability (i.e., a threshold energy resource level), and C_{ep} is a parameter which models the effects of the cooler marine environment on the performance of FPV systems. C_{ep} is expressed as (Marion, 2010):

$$C_{ep} = 1 + \alpha_P (T_C - T_{STC}), \tag{3}$$

where $\alpha_P = -0.36$ % °C^{-1} is the PV system temperature coefficient of power (Martínez and Iglesias, 2024a), T_C is the spatial distribution of the operating temperature of the PV system, and $T_{STC} = 25$ °C stands for the operating temperature at standard test conditions (López, M. et al., 2022). In the present application, T_C is modelled by (Kalogirou, 2023):

$$T_C = 30 + 0.0175 \times (E_g - 300) + 1.14 \times (T_a - 25), \tag{4}$$

being T_a the spatial distribution of the ambient temperature, which is obtained from the Copernicus Climate Change Service (C3S) and computed by the European Centre for Medium-Range Weather Forecasts (ECMWF) reanalysis products (ERA5) for the period 1991–2020 (Hersbach et al., 2020).

In this work, E_g is retrieved from PVGIS (Photovoltaic Geographical Information System), a web GIS tool widely used for the analysis of PV technology in Europe (Huld et al., 2012). This tool stores solar radiation data obtained from satellite operation. In particular, the present application resorts to CMSAF (Climate Monitoring Satellite Application Facility) data (Schulz et al., 2009), based on Meteosat geostationary satellite images which are processed to obtain different GHI datasets (Amillo et al., 2014). Likewise, $E_{g,ref}$ is set to 100 Wm^{-2} (Yang et al., 2024). The period of interest for the analysis of E_g can be adapted (e.g., shorter time periods, such as seasonal or monthly scenarios), similar to $E_{g,ref}$.

As mentioned, the SE index indicates suitability for solar energy exploitation in areas where SE $\geq$ 1. The upper limit of the SE index (and thus of the IFSE index) is expected to be about 2.5, which would correspond with desertic areas with a GHI of about 250 Wm^{-2}. As a result, this dimensionless metric constitutes a reliable indicator for the assessment of the exploitability of the solar energy resource at coastal locations of interest.

3.2. Application of the SE index to the Ría de Vigo

On the basis of the above procedure (Section 3.1), the spatial distribution of the SE index in the Ría Vigo is computed (Fig. 4). As can be observed, it is virtually homogeneous within the whole coastal area, mainly as a consequence of the reduced spatial variations of E_g (Fig. 3), ranging between 1.8 and 2.0, and reaching its maximum value in the surroundings of the Baiona Bay (located in the southern margin of the ria, closer to its mouth, and limited by Cape Silleiro and Punta Lameda).

Given the homogeneity of the SE index, the spatial distribution of the IFSE index, and therefore the identification of the most appropriate locations for solar energy exploitation in the Ría de Vigo, are expected to be highly dependent on the spatial distribution of the installation costs ($C_{gp,s}$, Section 4) and water uses (U_{gp}, Section 5) within the ria.

4. Geospatial cost penalty function ($C_{gp,s}$)

4.1. Development of $C_{gp,s}$

The next step involves adapting the geospatial cost penalty function (previously C_{gp}) to the technical requirements of solar energy exploitation, denoted as $C_{gp,s}$. This new function, independent of a specific FPV technology or layout, identifies and penalises coastal areas where the deployment of FPV systems would incur larger installation costs by means of a detailed parameterisation of the main capital expenditures (CAPEX) as a function of the geomorphological parameters on which they depend.

The CAPEX encompasses the expenses incurred during the construction or fabrication and installation of an industrial facility or, in other words, prior to its operation stage. In the case of marine renewable energy projects, this cost term usually groups the expenses of (Dalton et al., 2015): (i) energy conversion technology, (ii) cabling, (iii) foundations or moorings and anchors, (iv) deployment procedure, and (v) electrical grid connection. More specifically, the influence of the coastal configuration on CAPEX has been thoroughly studied in previous works for the particular case of marine renewable energy projects, identifying cabling and mooring as the main CAPEX drivers with a strong dependence on geomorphological aspects such as water depth and shoreline distance (Fouz et al., 2022). Therefore, these CAPEX terms and geomorphological variables are retained in this work for the development of $C_{gp,s}$.

Cable costs are usually subdivided into inter-array cable, which connects the different strands and floating structures of a specific FPV plant layout, and exporting cable, which transports the energy yield to an onshore substation (Martínez and Iglesias, 2024b). The first is outside the scope of this work given that it is highly dependent on the specific farm layout, which contradicts the technology-agnostic aim of the IFSE index. Exporting cable costs (hereinafter, cable costs), C_{ec}, can be parametrised as a function of shoreline distance, being computed as (Martínez and Iglesias, 2024b):

$$C_{ec} = l_{ec} C_{u,ec} P_T \approx l C_{u,ec} P_T, \tag{5}$$

where l_{ec} is the total cable length, which is accurately approximated by the shoreline distance, l, $C_{u,ec}$ represents the unitary cost per unity of cable length and installed power ($C_{u,ec} = 2.18$ € (MW m)$^{-1}$), and P_T stands for the total plant power.

Mooring costs include the expenses of both mooring lines and anchorages required for limiting the movements of floating platforms ensuring their structural stability. Given their easily manufacturing and economic feasibility, recent works resort to tension-legged substructures composed by four taut mooring lines and the corresponding anchorage points constituted by concrete dead weights in the form of gravity anchors (Martínez and Iglesias, 2024b). Thus, the cost of mooring and anchoring, C_{ma}, is calculated as the sum of the costs of the mooring lines, C_m, and anchoring system, C_a, as follows (Martínez and Iglesias, 2024b):

$$C_{ma} = C_m + C_a = l_{ml} C_{u,ml} N_{ml} N_{fs} + W_{u,dw} C_{u,dw} N_{dw} N_{fs}, \tag{6}$$

where l_{ml} is the length of mooring lines, which is computed as the water depth adjusted by a generic draft for FPV installations, $C_{u,ml}$ represents the cost per unity of length for the mooring lines ($C_{u,ml} = 57.6$ €m^{-1}), N_{ml} stands for the number of mooring lines per floating structure, N_{fs} is the number of floating structures, $W_{u,dw}$ represents the unitary weight per unit of concrete dead weights ($W_{u,dw} = 23$ ton), $C_{u,dw}$ stands for the cost per unit of weight for the concrete dead weights ($C_{u,dw} = 44$ €ton^{-1}), and N_{dw} is the number of concrete dead weights per substructure.

Therefore, the total plant CAPEX function, C_{plant} (€), can be computed by combining and rearranging Eqs. (5) and (6) as:

$$C_{plant} = C_{ec} + C_{ma} = \beta l + \gamma N_{fs} d + \delta N_{fs}, \tag{7}$$

where $\beta = C_{u,ec} P_T$, $\gamma = 230.4$ and $\delta = 1398.4$ are coefficients that result of rearranging the constant terms in Eqs. (5) and (6), and d represents the water depth (i.e., the real water depth, given the effects of the abovementioned draft adjustment are modelled by γ and δ).

The influence of the coastal configuration —defined by its most representative parameters, i.e., water depth, d, and shoreline distance, l— on the total CAPEX is illustrated by Eq. (7). Nevertheless, and despite its interest, Eq. (7) depends on site-specific parameters resulting from a detailed plant layout (i.e., P_T and N_{fs}), which require explicit definition, and therefore does not represent all possible FPV system configurations. To ensure that the resulting function will be broadly applicable to any FPV system deployed in any coastal area of interest, these site-specific parameters should be standardised, for which the following approach is applied.

Both parameters, P_T and N_{fs}, are closely interconnected. Once the total plant power is established, the required number of PV panels to achieve this power must be determined, which in turn determines the necessary number of floating structures to support them. Some of the issues involved in defining these technical aspects may be unclear at early project stages, so the current trends and prospects of FPV technology should be carefully considered to ensure the reliable standardisation of the site-specific parameters (i.e., P_T and N_{fs}). In this regard, based on previous works, and with a particular emphasis on FPV operation in nearshore coastal environments, a total plant power $P_T = 1$ MW is retained for further analyses (Trapani and Redón Santafé, 2015).

Regarding the number of floating structures required to support the number PV panels necessary to achieve the total plant power (i.e., 1 MW), it strongly depends on the final layout of the array (e.g., number of rows and columns, arrangement of the different strands, etc.), and therefore is also dependent on the site-specific availability of useable surface in a given coastal area, which in turn is highly influenced by the coastal configuration and the interactions among the different water uses. Thus, its definition constitutes a complex task if conducted with independence of the final layout. To avoid this complexity, in this work a wide range of real FPV projects is considered in order to accurately characterise the relation between the total plant power and the number of floating structures required to support the number of PV panels necessary to attain it (Islam et al., 2023; López, M. et al., 2024; Martínez and Iglesias, 2024a, 2024b; Trapani and Redón Santafé, 2015). Once conducted this analysis, the results are parametrised by unit of installed power, and N_{fs} can be obtained as a generic parameter (i.e., number of floating structures per MW of installed power) to be applied to FPV projects at early stage.

Thus, the standardisation of the site-specific parameters as described, leads to the generalisation of Eq. (7). The generalised total CAPEX function, $C_{plant,g}$ (€), is obtained after the operation and rearrangement of the terms in Eq. (7), which now reads:

$$C_{plant,g} = \beta_g l + \gamma_g d + \delta_g, \tag{8}$$

where $\beta_g = 2.18$, $\gamma_g = 3456$ and $\delta_g = 20976$ are the constant coefficients

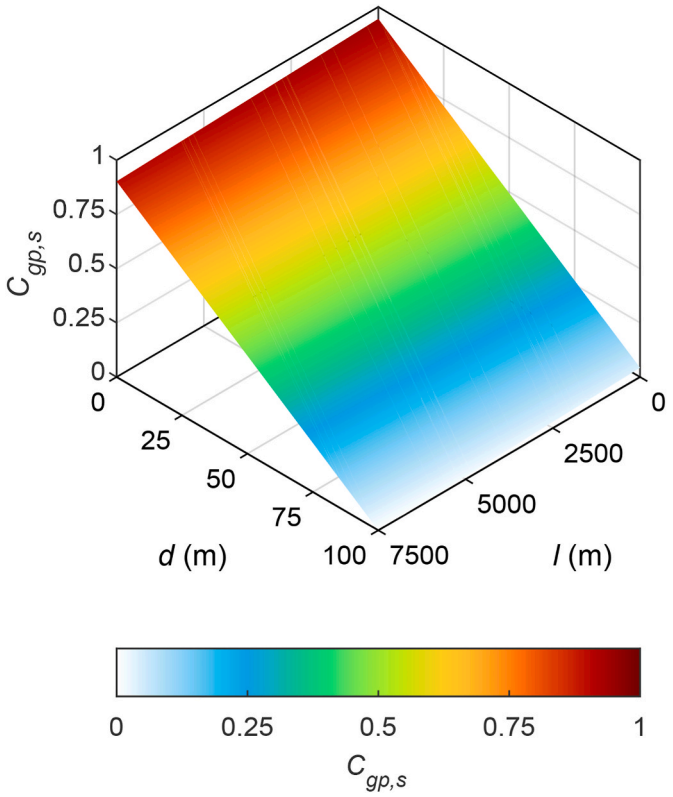

Fig. 5. Representation of $C_{gp,s}$ (Eq. (9)) for a generic domain.

resulting from generalising and rearranging the constant terms in Eqs. (5) and (6).

Eq. (8) provides a generalised expression applicable to any coastal area of interest, enabling an estimated assessment of CAPEX based on the shoreline distance and water depth at any given site. Building upon this, the geospatial cost penalty function, now adapted for solar energy exploitation through FPV technology, $C_{gp,s}$, establishes a relationship between the installation costs and geomorphological aspects (i.e., shoreline distance and water depth), being expressed as:

$$C_{gp,s} = 1 - \frac{C_{plant,g}}{C_{plant,g,ref}}, \tag{9}$$

where $C_{plant,g,ref}$ is a threshold value for Eq. (8), beyond which energy conversion becomes unfeasible, resulting from a large shoreline distance, water depth, or a combination of both factors. Based on previous works, the limiting value for the shoreline distance is set to $l = 7500$ m (Carballo et al., 2024), and in the case of water depth, $d = 100$ m according to specific developments for FPV technology (Garrod et al., 2024). In addition, areas not suited for FPV systems, i.e., very close to the shoreline or with reduced water depths ($l < 500$ m or $d < 2$ m) are disregarded.

Fig. 5 shows the representation of $C_{gp,s}$ (Eq. (9)) for a generic domain

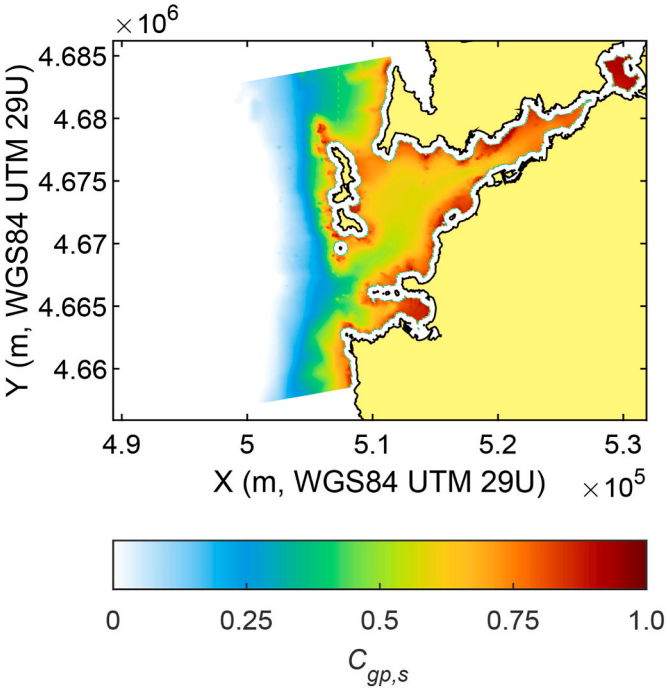

Fig. 7. Spatial distribution of $C_{gp,s}$ throughout the Ría de Vigo.

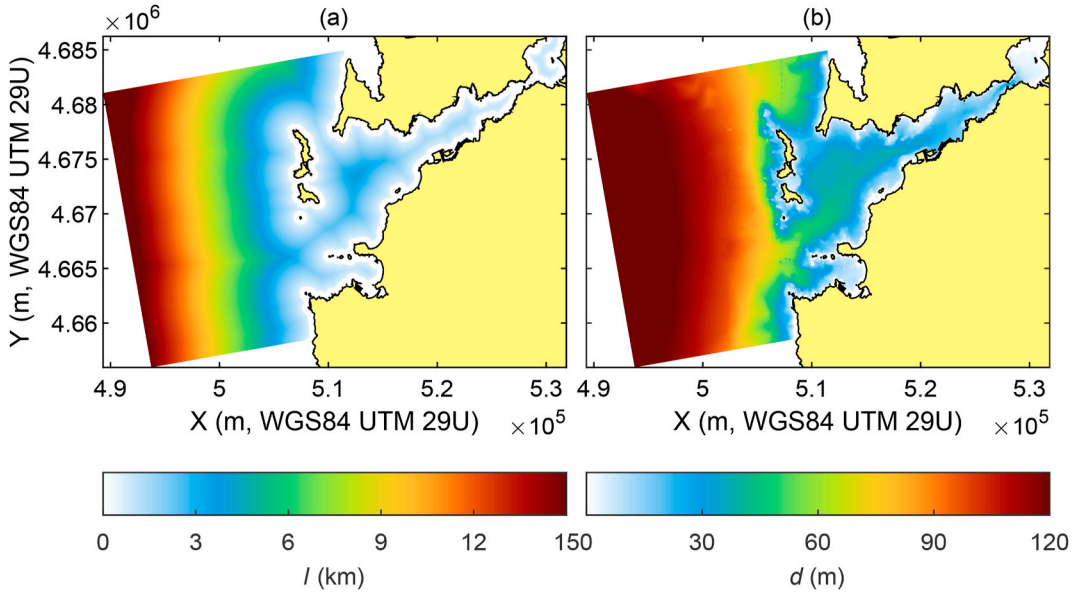

Fig. 6. Spatial distribution of the shoreline distance (a) and water depth (b) throughout the Ría de Vigo.

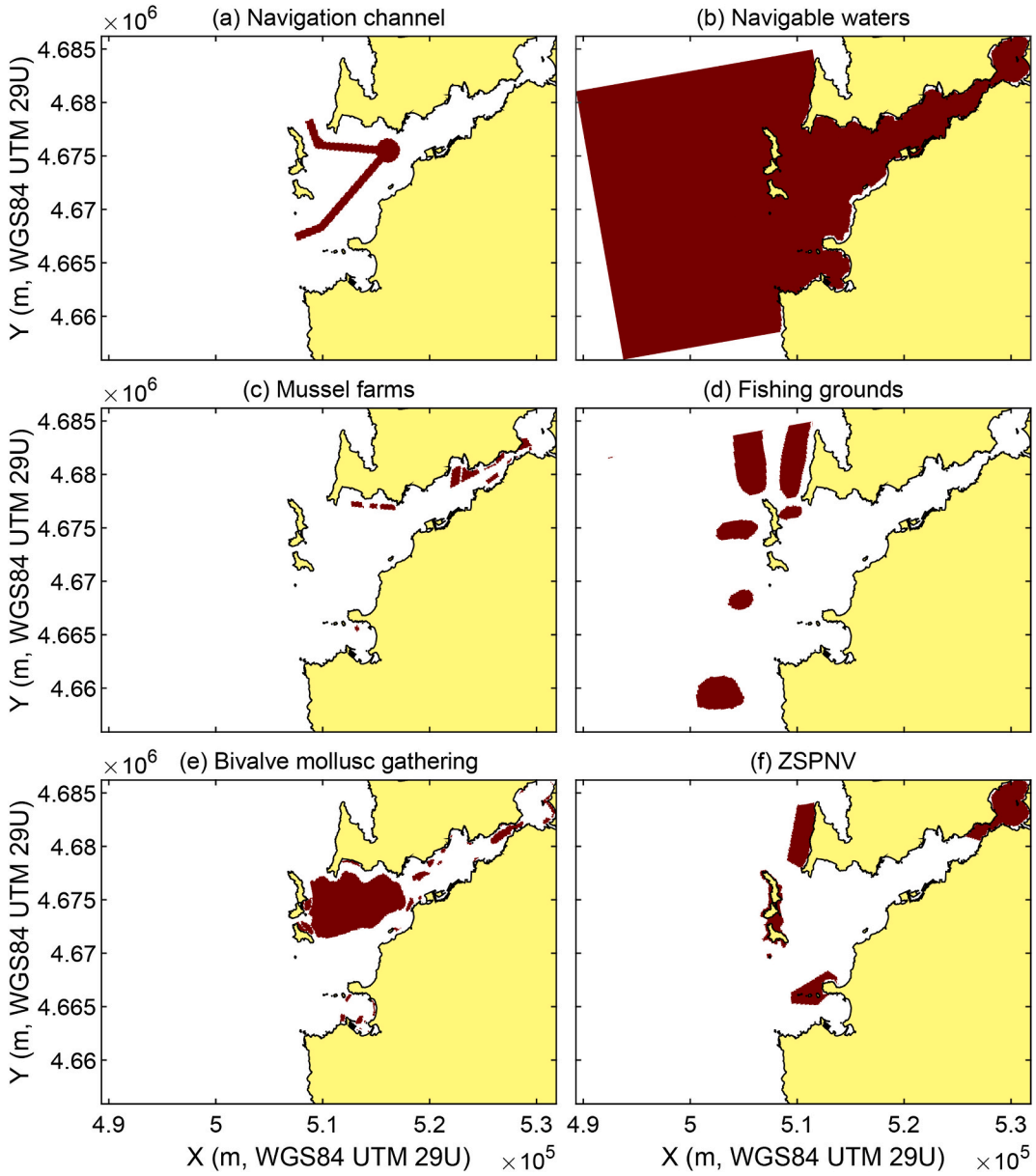

Fig. 8. Spatial distribution of the main water uses throughout the Ría de Vigo.

up to the abovementioned limiting values for shoreline distance and water depth. As can be observed, the water depth has a more important role as CAPEX driver than the shoreline distance resulting from $\gamma_g \gg \beta_g$ (Eq. (8)). On the other hand, it is important to note that $\delta_g > 0$ (Eq. (8)) and thus there always exist a reduced penalisation, i.e., $C_{gp,s} < 0.95$, which results from the installation of FPV systems instead of GPV technology, even in an idealised location where $l = d \approx 0$, which could correspond with a port or a specific site at the shoreline.

4.2. Application of $C_{gp,s}$ to the Ría de Vigo

Fig. 6 illustrates the spatial distribution of the shoreline distance and water depth in the Ría de Vigo, required for the computation of $C_{gp,s}$ shown in Fig. 7. As a result of the coastal configuration, the largest penalisation takes place in the surroundings of the mouth of the ria, and increasing to the west of Cíes Islands, where $C_{gp,s}$ figures of less than 0.25 are found. On the other hand, the inner and middle ria are less restrictive according to their geomorphological conditions resulting in an overall lower penalisation (i.e., $C_{gp,s}$ of approx. 0.7–0.8). However, specific areas such as the deeper central channel in the middle ria, present significant higher penalisation ($C_{gp,s} \approx 0.5$–0.6).

5. Geospatial water use penalty function (U_{gp})

5.1. Development of U_{gp}

The last step towards the development of the IFSE index is the computation of the geospatial cost penalty function, U_{gp}. In this case, given it considers socioeconomic and environmental aspects directly resulting from a multicriteria characterisation of the area of interest (i.e., independent of the energy conversion technology considered), no specific adaptations are required for its straightforward application to solar energy analysis.

U_{gp} provides a reliable indicator to assess the coexistence between energy exploitation and the surrounding existing or potential coastal uses. Two different steps are required for its computation: (i) the identification and characterisation of the main socioeconomic (e.g., fishing, shipping, etc.) and environmental (e.g., protected areas, such as Natura

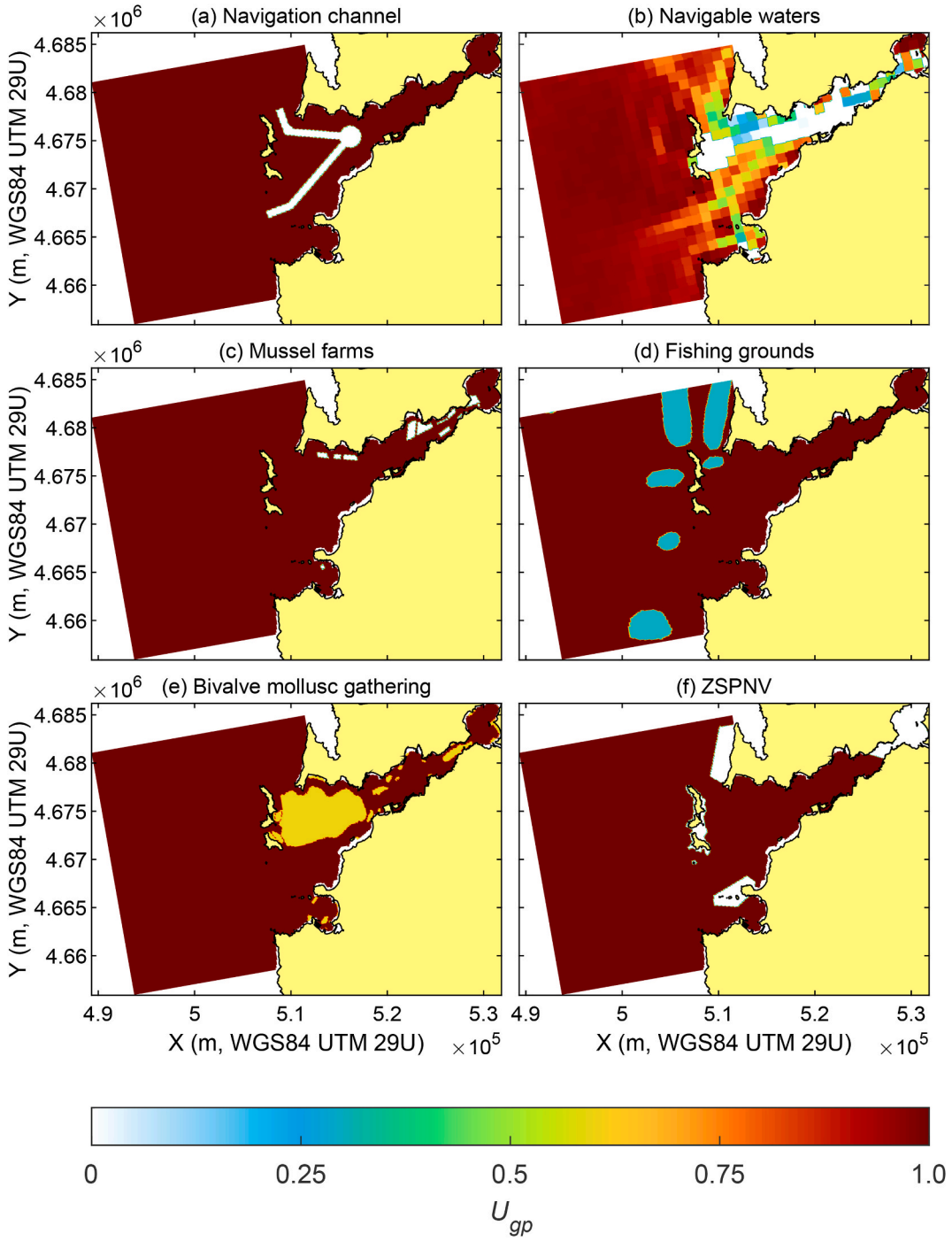

Fig. 9. Spatial distribution of U_{gp} values for each main water use considered.

2000 Network) water uses, and (ii) their quantitative assessment, defining the value of U_{gp} function in these areas. Finally, if a superposition of uses is present in a given area, specific aggregation methods should be defined. In the present work, the most restrictive value of U_{gp} (i.e., the minimum) is retained (Carballo et al., 2024). An alternatively method could consist in adding the various penalisation up to a limiting value of $U_{gp} = 0$. The quantitative assessment of the U_{gp} function for the different coastal uses identified (step ii) is not straightforward and requires a comprehensive approach adapted to the specific characteristics of each coastal use. For the sake of simplicity, the reader is referred to previous works (e.g., Fouz et al., 2022) for further details regarding the definition of U_{gp} for each specific use.

Regarding the particular case of the Ría de Vigo, it hosts a large number of socioeconomic and environmental water uses, highlighting the intense activity taking place in the Port of Vigo, one of the most important port areas in northern Spain in terms of maritime transport (e.g., shipping containers) and fishing, along with the high environmental value of the Cíes archipelago. Moreover, the comprehensive work conducted by the Port Authority of Vigo (APVigo), which manages several port facilities within the ria, makes available a large amount of geospatial data relative to port activities and zoning, which are suitable for being analysed through the U_{gp} function.

As a result, the following water uses are considered in this work. On the one hand, as socioeconomic activities: (i) shellfishing, (ii) mussel farms (i.e., traditional rafts for its cultivation), (iii) bivalve mollusc gathering (i.e., other species, such as oysters or clams), (iv) fishing

Table 1
U_{gp} values considered for socioeconomic and environmental water uses in the Ría de Vigo.

Water use	U_{gp}
Shellfishing	0.30
Ferry routes	0
Anchoring zones	0
Port zone I	0
Natura 2000 Network	0.90
National Parks	0

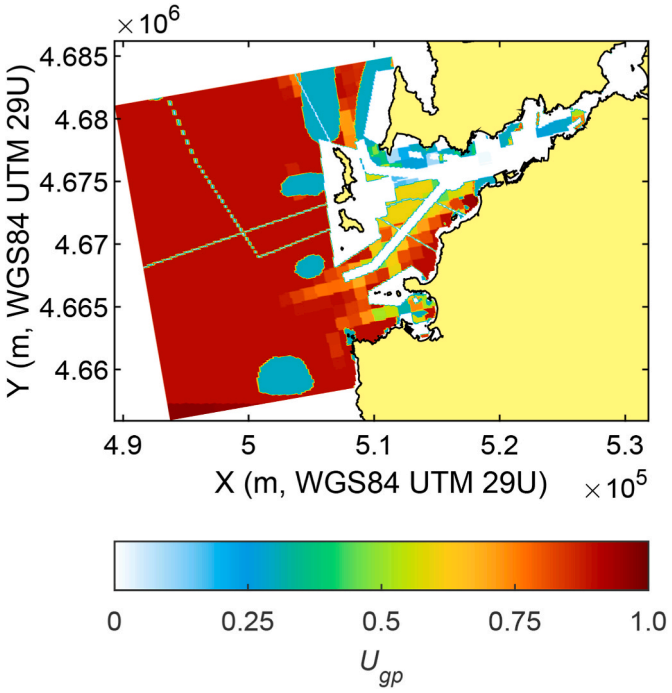

Fig. 10. Spatial distribution of U_{gp} throughout the Ría de Vigo.

grounds, (v) navigable waters and/or navigation channels, (vi) ferry routes, (vii) anchoring zones (i.e., those delimited and managed by APVigo), and finally, (viii) port zone I (i.e., the public water surface comprising the interior of harbour waters, including all areas that are sheltered either naturally or by the effect of seawalls, managed by APVigo). On the other hand, as environmental aspects: (i) Natura 2000 Network (ii) National Parks (i.e., a protection figure from the Spanish legal framework, such as Cíes archipelago), and (iii) Zones of Special Protection of Natural Values (ZSPNV) (i.e., a regional protection figure which applies to those areas whose natural, cultural, scientific, educational or landscape value makes it necessary to ensure their conservation and which do not have any other specific protection; however, in the particular case of Galicia, it also includes the Natura 2000 Network, being overlapped in extensive areas).

For the sake of simplicity, Figs. 8 and 9 show the spatial distribution of the main water uses in the Ría de Vigo and their resulting U_{gp} value, respectively. The U_{gp} values for all considered water uses are presented in Table 1.

5.2. Application of U_{gp} to the Ría de Vigo

The spatial distribution of U_{gp} in the Ría de Vigo, computed as introduced in Section 5.1, is shown in Fig. 10. As a result of the high number of water uses coexisting in the Ría de Vigo, a large part of the inner and middle ria is considered as a restricted area (i.e., $U_{gp} = 0$), where the energy exploitation is incompatible with the existing socioeconomic and environmental restraints. On the contrary, there is a large area in the outer ria, closer to its south margin, and in particular to the south of the southernmost branch of the navigation channel, between Cape do Mar and Punta Lameda, which presents medium to high U_{gp} values (i.e., $U_{gp} \approx 0.6$–0.9), indicating suitability for energy exploitation. Likewise, there are specific areas also located in the Soth margin of the mouth of the Ría, in the surroundings of the Baiona Bay, which also present similar figures of U_{gp} parameter.

6. IFSE index

The integration of the different terms constituting the IFSE index (i.e., SE in Section 3, $C_{gp,s}$ in Section 4, and U_{gp} in Section 5) leads to the computation of its spatial distribution in the Ría de Vigo following Eq. (1). Its physical interpretation, as previously introduced, is straightforward: the higher the IFSE index, the better the site for solar energy exploitation, with IFSE $\geq$1 indicating suitability. In consequence, IFSE = 1 would represent a suitability threshold indicating locations with a minimum level of energy resource (i.e., SE = 1), and without

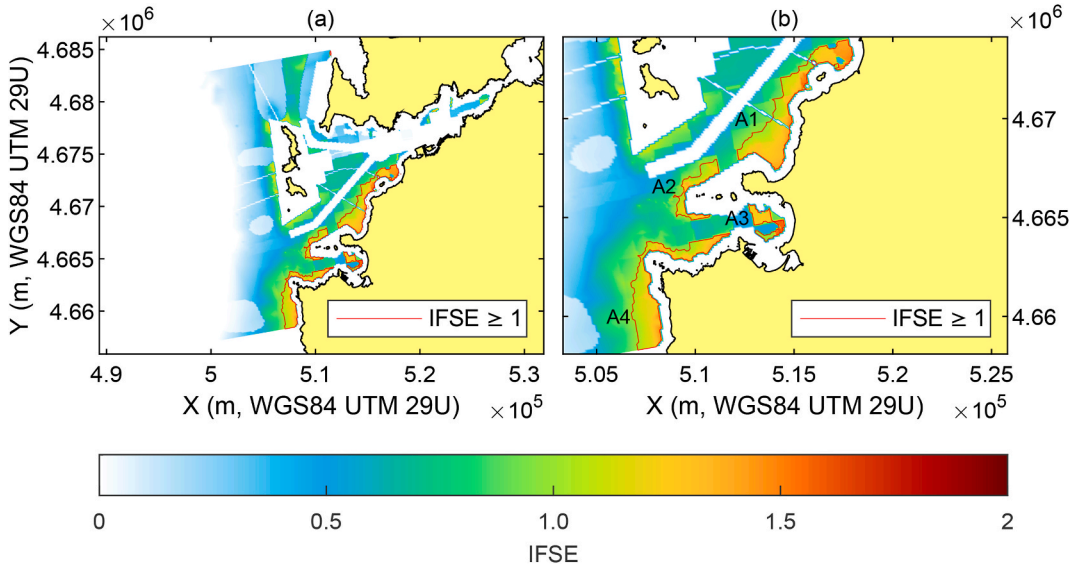

Fig. 11. Spatial distribution of the IFSE index (a) and the resulting areas of interest (A1 to A4) (b).

Table 2
Characteristic values of the IFSE index in the areas identified as of interest (A1 to A4) and their main characteristics [surface (S), mean value of the IFSE index ($IFSE_{mean}$), maximum value of the IFSE index ($IFSE_{max}$), standard deviation of the IFSE index (σ_{IFSE}), mean water depth (d_{mean}), maximum water depth (d_{max}), standard deviation of the water depth (σ_d)].

Area	S (km^2)	$IFSE_{mean}$	$IFSE_{max}$	σ_{IFSE}	d_{mean} (m)	d_{max} (m)	σ_d (m)	Seabed type
A1	7.98	1.24	1.56	0.13	19.03	33.54	6.23	Stone and gravel
A2	1.73	1.15	1.46	0.08	25.18	35.32	4.29	Stone
A3	1.11	1.26	1.61	0.18	9.08	13.00	1.71	Stone and gravel
A4	6.19	1.18	1.52	0.10	25.31	38.11	6.42	Stone and gravel

penalisations in terms of installation costs (i.e., $C_{gp,s} = 1$) and coexistence with other water uses (i.e., $U_{gp} = 1$).

The spatial distribution of the IFSE index in the Ría de Vigo, with the areas where IFSE $\geq$1 (i.e., suitable for energy exploitation) is shown in Fig. 11. The main characteristics of these areas are summarised in Table 2.

The results of the IFSE index throughout the Ría de Vigo reveal a total of four large areas suitable for the installation of FPV systems (Areas A1 to A4). These areas, which had not been identified in previous research, are located off the southern margin of the outer ria: Area A1 (branch between cape Estay and Punta Lameda), Area A2 (surroundings of Illas Serralleiras), Area A3 (in front of Baiona Bay) and Area A4 (mouth of the Ría in the surroundings of Cape Silleiro). The most suited areas in terms of IFSE index correspond with Areas A1 and A3 with an average IFSE index of about 1.24 and 1.26, respectively, followed by Areas A2 and A4 with slightly lower values, of 1.15 and 1.18, respectively. In addition, there is a rather spatial stability in the IFSE index figures throughout all the areas interest, with standard deviations of the IFSE index of about 0.1, and with somewhat greater values in the locations closer to the coast. Despite the similar average values of IFSE, these areas present also significant differences, in particular with respect to the total surface available and water depth. First, Areas A1 and A4 present a much greater available surface with about 8 and 6 km^2, respectively, than Areas A2 and A3, with about 1–2 km^2. Regarding the water depth, Areas A2 and A4 present greater values with an average depth of about 25 m, followed by Area A1 with approx. 19 m, and finally Area A3 with only 9 m, as a result of it being located in front of the Baiona Bay. In addition, other aspects such as the sheltering effect of the coastal configuration on the wave action may be also of interest, not being included in the computation of IFSE index computation —as it is the case of the available surface—. Based on all the aspects considered, it may be established that Area A1 emerges as that with greater interest, being that with greater IFSE index and area available, with similar values to Area A4, but significantly less exposed to wave action. Despite Area A1 being that with higher interest, the remaining areas also present interest for the operation of FPV systems.

7. Conclusions

The main challenge at early stages of marine renewable energy projects is the large number of uncertainties involved in the decision-making processes. To address this challenge, several novel indices have been recently proposed for the various marine renewable energy resources, such as wind, wave or hydrokinetic energy. Such an index was lacking for floating solar energy. In this work, the new IFSE (Integrated Floating Solar Energy) index is proposed and developed for siting FPV technology in coastal areas, with a particular focus on estuarine areas. This index follows a similar approach to the IHE (Integrated Hydrokinetic Energy) index, developed for identifying the coastal areas most suitable for hydrokinetic energy exploitation. Finally, the resulting index is applied to the case study of the Ría de Vigo, an estuary located in NW Spain, characterised by its sheltered conditions resulting from the natural barrier constituted by the Cíes Islands, and whose favourable environmental conditions for FPV operation have been highlighted in previous works.

The development of the IFSE index is conducted in different stages. First, the distribution of the solar energy resource is assessed through the SE (solar energy) index, which characterises the suitability of coastal areas for SE exploitation from the point of view of the exploitability of the energy resource. SE values greater than 1 indicate suitability for FPV system operation without considering further restrictions (coastal configuration and water uses). Then, the geospatial cost penalty function, $C_{gp,s}$ and the geospatial water use penalty function, U_{gp}, are developed, with values ranging from 1 (no restriction) to 0 (total restriction). $C_{gp,s}$ is applied to assess the costs of installation of a FPV facility considering the coastal configuration, and in particular the water depth and the distance to the coast. Then, the geospatial water use penalty function, U_{gp}, is used to determine the suitability of a location for a FPV facility according to its coexistence with preexisting or potential socioeconomic activities or environmental factors. Finally, the geospatial distribution of the IFSE index is obtained by multiplying SE, $C_{gp,s}$ and U_{gp} terms. As a result, locations with an IFSE index larger than 1 are suitable for FPV system operation, with greater values indicating better conditions for their operation.

The spatial distribution of the IFSE index throughout the Ría de Vigo reveals four large areas suitable for the installation of FPV systems, Areas A1 to A4, located off the southern margin of the outer ria. Amongst them, Area A1 seems to emerge as that with the highest interest, based on its greater IFSE index ($IFSE_{mean} = 1.24$) and area available (6.98 km^2), presenting similar values to Area A4, but being subject to a less harsh wave climate. All in all, the four identified areas are suitable for FPV farms.

The present methodology and the results obtained for the Ría de Vigo demonstrate how the IFSE index can serve as a decision-aid tool for delimiting the areas of interest for installing FPV systems in coastal areas, significantly improving on existing procedures and mitigating the uncertainties at the early stages of these projects. In future work, the IFSE index will be extended to consider the wave field for evaluating the costs of installation and operation, thereby increasing its accuracy for its application to coastal areas exposed to wave action. Finally, it is necessary to highlight that the IFSE index aims to address uncertainties involved in the decision-making processes at early stages of FPV projects. Thus, the final FPV farm design would require a detailed cost analysis considering the different possible combination of technologies and array distribution.

CRediT authorship contribution statement

D.M. Fouz: Writing – original draft, Visualization, Methodology, Investigation, Formal analysis, Conceptualization. **R. Carballo:** Writing – review & editing, Supervision, Methodology, Investigation, Funding acquisition, Conceptualization. **I. López:** Writing – review & editing, Visualization, Methodology, Formal analysis. **B. Álvarez:** Writing – original draft, Methodology, Investigation, Formal analysis. **G. Iglesias:** Writing – review & editing, Supervision, Methodology, Conceptualization.

Declaration of competing interest

The authors declare that they have no known competing financial

interests or personal relationships that could have appeared to influence the work reported in this paper.

Acknowledgements

This work was supported by 'Axudas para a consolidación e estruturación de unidades de investigación competitivas e outras accións de fomento nas universidades do Sistema Universitario de Galicia (2023-25)' with reference number ED431B 2023/17.

During this work D.M. Fouz was supported by the postdoctoral orientation period of a predoctoral grant of the 'Convocatoria de contratos predoutorais do Campus de Especialización Campus Terra' with reference number 8042 272B 64100 and 'Axudas para a consolidación e estruturación de unidades de investigación competitivas e outras accións de fomento nas universidades do Sistema Universitario de Galicia (2025-28)' with reference number ED431C 2025/17.

Nomenclature

Abbreviation	Meaning
FPV	Floating solar photovoltaic
PV	Solar photovoltaic
GPV	Ground-mounted solar photovoltaic
LCOE	Levelized costs of energy
R&D	Research and development
W	West
NW	Northwest
N	North
GHI	Global horizontal irradiance
S&E	Socioeconomic and environmental
C3S	Copernicus Climate Change Service
ECMWF	European Centre for Medium-Range Weather Forecasts
PVGIS	Photovoltaic Geographical Information System
CMSAF	Climate Monitoring Satellite Application Facility
CAPEX	Capital expenditures
APVigo	Porth Authority of Vigo
ZSPNV	Zones of Special Protection of Natural Values

Symbols	Meaning
€/kWh	Euros per kilowatt-hour
Wm^{-2}	Watts per square meter
°C	Degrees Celsius
$(MW\ m)^{-1}$	Megawatt per meter

Variables	Meaning	Units
IHE	Integrated Hydrokinetic Energy	Dimensionless
IFSE	Integrated Floating Solar Energy	Dimensionless
C_{gp}	Geospatial cost penalty function	Dimensionless
U_{gp}	Geospatial water use penalty function	Dimensionless
SE	Solar Energy resource index	Dimensionless
$C_{gp,s}$	Geospatial cost penalty function adapted to solar energy exploitation	Dimensionless
E_g	Yearly averaged value of the GHI over a horizontal surface considering all time	Wm^{-2}
$E_{g,ref}$	Threshold value for E_g (minimum energy resource required for energy exploitation)	Wm^{-2}
C_{ep}	Cooling effects parameter	Dimensionless
α_P	PV system temperature coefficient of power	$\%\ °C^{-1}$
T_C	Spatial distribution of the operating temperature of the PV system	°C
T_{STC}	Operating temperature at standard test conditions	°C
T_a	Spatial distribution of the ambient temperature	°C
C_{ec}	Exporting cable costs	€
l_{ec}	Exporting cable length	m
$C_{u,ec}$	Unitary cost for exporting cable per unity of cable length and installed power	$(MW\ m)^{-1}$
P_T	Total plant power	MW
l	Shoreline distance	m
C_{ma}	Cost of mooring and anchoring	€
C_m	Cost of mooring	€
C_a	Cost of anchoring	€
l_{ml}	Length of mooring lines	m
$C_{u,ml}$	Cost per unity of length for the mooring lines	$€m^{-1}$
N_{ml}	Number of mooring lines per floating structure	Dimensionless
N_{fs}	Number of floating structures	Dimensionless
$W_{u,dw}$	Unitary weight per unit of concrete dead weights	ton
$C_{u,dw}$	Cost per unit of weight for the concrete dead weights	$€ton^{-1}$
N_{dw}	Number of concrete dead weights per substructure	Dimensionless
C_{plant}	Total plant CAPEX function	€
β	Coefficient for exporting cable (Eq. (7))	$€m^{-1}$
γ	Coefficient for moorings and anchoring (Eq. (7))	$€m^{-1}$
δ	Coefficient for moorings and anchoring (Eq. (7))	Dimensionless
d	Water depth	m
$C_{plant,g}$	Generalised total plant CAPEX function	€
β_g	Generalised coefficient for exporting cable (Eq. (8)	$€m^{-1}$
γ_g	Generalised coefficient for moorings and anchoring (Eq. (8))	$€m^{-1}$
δ_g	Generalised coefficient for moorings and anchoring (Eq. (8))	Dimensionless

(continued on next page)

(*continued*)

$C_{plant,g,ref}$	Threshold value for $C_{plant,g}$ (beyond which energy conversion becomes unfeasible)	€
S	Surface	km^2
$IFSE_{mean}$	Mean value of the IFSE index	Dimensionless
$IFSE_{max}$	Maximum value of the IFSE index	Dimensionless
σ_{IFSE}	Standard deviation of the IFSE index	Dimensionless
d_{mean}	Mean value of the water depth	m
d_{max}	Maximum value of the water depth	m
σ_d	Standard deviation of the water depth	m

Data availability

Data will be made available on request.

References

Amillo, A.G., Huld, T., Müller, R., 2014. A new database of global and direct solar radiation using the Eastern Meteosat satellite, models and validation. Remote Sens. 6 (9), 8189. https://doi.org/10.3390/rs6098165.

Bahaj, A.S., Mahdy, M., Alghamdi, A.S., Richards, D.J., 2020. New approach to determine the importance index for developing offshore wind energy potential sites: supported by UK and Arabian Peninsula case studies. Renew. Energy 152, 441–457. https://doi.org/10.1016/j.renene.2019.12.070.

Carballo, R., Fouz, D.M., López, I., Iglesias, G., 2024. Hydrokinetic energy site selection under high seasonality: the i-IHE index. Renew. Energy 237, 121695. https://doi.org/10.1016/j.renene.2024.121695.

Claus, R., López, M., 2022. Key issues in the design of floating photovoltaic structures for the marine environment. Renew. Sustain. Energy Rev. 164, 112502. https://doi.org/10.1016/j.rser.2022.112502.

Claus, R., López, M., 2023. A methodology to assess the dynamic response and the structural performance of floating photovoltaic systems. Sol. Energy 262, 111826. https://doi.org/10.1016/j.solener.2023.111826.

Dalton, G., Allan, G., Beaumont, N., Georgakaki, A., Hacking, N., Hooper, T., Kerr, S., O'Hagan, A.M., Reilly, K., Ricci, P., Sheng, W., Stallard, T., 2015. Economic and socio-economic Assessment Methods for Ocean Renewable Energy: Public and Private Perspectives. https://doi.org/10.1016/j.rser.2015.01.068.

deCastro, M., Lavidas, G., Arguilé- Pérez, B., Carracedo, P., deCastro, N.G., Costoya, X., Gómez-Gesteira, M., 2024. Evaluating the economic viability of near-future wave energy development along the Galician coast using LCoE analysis for multiple wave energy devices. J. Clean. Prod. 463, 142740. https://doi.org/10.1016/j.jclepro.2024.142740.

Elminshawy, N.A.S., Ahmed, A., Osama, A., Kabeel, A.E., Elbaksawi, O., 2024a. The potential of optimized floating photovoltaic system for energy production in the Northern Lakes of Egypt. Eng. Anal. Bound. Elem. 161, 226–246. https://doi.org/10.1016/j.enganabound.2024.01.022.

Elminshawy, N.A.S., Osama, A., Gagliano, A., Oterkus, E., Tina, G.M., 2024b. A technical and economic evaluation of floating photovoltaic systems in the context of the water-energy nexus. Energy 303, 131904. https://doi.org/10.1016/j.energy.2024.131904.

Fang, Z., Xue, S., Cheng, C., Zhou, Q., Ali, M., Xu, R., Xu, J., Ding, T., Wang, J., Huang, Z., Sun, X., Bai, Y., 2024. Framework of land use planning for an energy producing city of Northwest China based on water-energy-food nexus. J. Clean. Prod. 451, 142126. https://doi.org/10.1016/j.jclepro.2024.142126.

Filgueira-Vizoso, A., Cordal-Iglesias, D., Fernández-Blanco, C., Fernández-Mira, D., García-Diez, A.I., Castro-Santos, L., 2025. Economic feasibility of floating offshore solar farms. The case of study of the Levantine-Balearic region of Spain. Energy 324, 136025. https://doi.org/10.1016/j.energy.2025.136025.

Fouz, D.M., Carballo, R., López, I., González, X.P., Iglesias, G., 2023. A methodology for cost-effective analysis of hydrokinetic energy projects. Energy 282, 128373. https://doi.org/10.1016/j.energy.2023.128373.

Fouz, D.M., Carballo, R., López, I., Iglesias, G., 2022. A holistic methodology for hydrokinetic energy site selection. Appl. Energy 317, 119155. https://doi.org/10.1016/j.apenergy.2022.119155.

Frías-Paredes, L., Gastón-Romeo, M., 2025. A new methodology to easy integrate complementarity criteria in the resource assessment process for hybrid power plants: offshore wind and floating PV. Energy Convers. Manag. X 26, 100938. https://doi.org/10.1016/j.ecmx.2025.100938.

Garrod, A., Neda Hussain, S., Ghosh, A., Nahata, S., Wynne, C., Paver, S., 2024. An assessment of floating photovoltaic systems and energy storage methods: a comprehensive review. Results Eng. 21, 101940. https://doi.org/10.1016/j.rineng.2024.101940.

Ghorbani, Y., Zhang, S.E., Nwaila, G.T., Bourdeau, J.E., Rose, D.H., 2024. Embracing a diverse approach to a globally inclusive green energy transition: moving beyond decarbonisation and recognising realistic carbon reduction strategies. J. Clean. Prod. 434, 140414. https://doi.org/10.1016/j.jclepro.2023.140414.

Hersbach, H., Bell, B., Berrisford, P., Hirahara, S., Horányi, A., Muñoz-Sabater, J., Nicolas, J., Peubey, C., Radu, R., Schepers, D., Simmons, A., Soci, C., Abdalla, S., Abellan, X., Balsamo, G., Bechtold, P., Biavati, G., Bidlot, J., Bonavita, M., Thépaut, J., 2020. The ERA5 global reanalysis. Q. J. R. Meteorol. Soc. 146 (730), 1999–2049. https://doi.org/10.1002/qj.3803.

Huang, J., Iglesias, G., 2024. Hybrid offshore wind–solar energy farms: a novel approach through retrofitting. Energy Convers. Manag. 319, 118903. https://doi.org/10.1016/j.enconman.2024.118903.

Huld, T., Müller, R., Gambardella, A., 2012. A new solar radiation database for estimating PV performance in Europe and Africa. Sol. Energy 86 (6), 1803–1815. https://doi.org/10.1016/j.solener.2012.03.006.

Islam, M.I., Jadin, M.S., Mansur, A.A., Kamari, N.A., Jamal, T., Hossain Lipu, M.S., Azlan, M.N., Sarker, M.R., Shihavuddin, A.S.M., 2023. Techno-economic and carbon emission assessment of a large-scale floating solar PV system for sustainable energy generation in support of Malaysia's renewable energy roadmap. Energies 16 (10). https://doi.org/10.3390/en16104034.

Kalogirou, S.A., 2023. Solar Energy Engineering: Processes and Systems. Elsevier.

López, I., Carballo, R., Fouz, D.M., Iglesias, G., 2024. Non-linear turbine selection for an OWC wave energy converter. Ocean Eng. 311, 118877. https://doi.org/10.1016/j.oceaneng.2024.118877.

López, M., Soto, F., Hernández, Z.A., 2022. Assessment of the potential of floating solar photovoltaic panels in bodies of water in mainland Spain. J. Clean. Prod. 340, 130752. https://doi.org/10.1016/j.jclepro.2022.130752.

López, M., Claus, R., Soto, F., Hernández-Garrastacho, Z.A., Cebada-Relea, A., Simancas, O., 2024. Advancing offshore solar energy generation: the HelioSea concept. Appl. Energy 359, 122710. https://doi.org/10.1016/j.apenergy.2024.122710.

Luhaniwal, J., Puppala, H., Agarwal, S., Mathur, T., 2024. Framework for strategic deployment of hybrid offshore solar and wind power plants: a case study of India. J. Clean. Prod. 479, 144009. https://doi.org/10.1016/j.jclepro.2024.144009.

Majidi, A.G., Ramos, V., Rosa-Santos, P., Akpınar, A., das Neves, L., Taveira-Pinto, F., 2025. Development of a multi-criteria decision-making tool for combined offshore wind and wave energy site selection. Appl. Energy 384, 125422. https://doi.org/10.1016/j.apenergy.2025.125422.

Marion, W., 2010. Overview of the PV Module Model in PVWatts (Presentation).

Martínez, A., Iglesias, G., 2024a. Floating solar photovoltaics in the Mediterranean Sea: mapping and sensitivity analysis of the levelised cost of energy. J. Clean. Prod. 473, 143534. https://doi.org/10.1016/j.jclepro.2024.143534.

Martínez, A., Iglesias, G., 2024b. Mapping of the levelised cost of energy from floating solar PV in coastal waters of the European Atlantic, North Sea and Baltic sea. Sol. Energy 279, 112809. https://doi.org/10.1016/j.solener.2024.112809.

Martínez, A., Iglesias, G., 2024c. Techno-economic assessment of potential zones for offshore wind energy: a methodology. Sci. Total Environ. 909, 168585. https://doi.org/10.1016/j.scitotenv.2023.168585.

Oliveira-Pinto, S., Stokkermans, J., 2020. Assessment of the potential of different floating solar technologies – overview and analysis of different case studies. Energy Convers. Manag. 211, 112747. https://doi.org/10.1016/j.enconman.2020.112747.

Peel, M.C., Finlayson, B.L., McMahon, T.A., 2007. Updated world map of the Köppen-Geiger climate classification. Hydrol. Earth Syst. Sci. 11 (5), 1633–1644. https://doi.org/10.5194/hess-11-1633-2007.

Penalba, M., Aizpurua, J.I., Martínez-Perurena, A., 2021. On the definition of a risk index based on long-term metocean data to assist in the design of Marine renewable energy systems. Ocean Eng. 242, 110080. https://doi.org/10.1016/j.oceaneng.2021.110080.

Rosa-Clot, M., Tina, G.M., 2020. Chapter 2 - current status of FPV and trends. In: Rosa-Clot, M., Marco Tina, G. (Eds.), Floating PV Plants. Academic Press, pp. 9–18. https://doi.org/10.1016/B978-0-12-817061-8.00002-6.

Sarkodie, S.A., Ahmed, M.Y., Owusu, P.A., 2023. Advancing COP26 climate goals: leveraging energy innovation, governance readiness, and socio-economic factors for enhanced climate resilience and sustainability. J. Clean. Prod. 431, 139757. https://doi.org/10.1016/j.jclepro.2023.139757.

Schulz, J., Albert, P., Behr, H.-., Caprion, D., Deneke, H., Dewitte, S., Durr, B., Fuchs, P., Gratzki, A., Hechler, P., Hollmann, R., Johnston, S., Karlsson, K.-., Manninen, T., M uller, R., Reuter, M., Riihel a, A., Roebeling, R., Selbach, N., Zelenka, A., 2009. Operational climate monitoring from space: the EUMETSAT satellite application facility on climate monitoring (CM-SAF). Atmos. Chem. Phys. 9 (5), 1687–1709. https://doi.org/10.5194/acp-9-1687-2009.

Thomas, B., Costoya, X., deCastro, M., Iglesias, G., Gómez-Gesteira, M., 2025. Levelized cost of energy for various floating offshore wind farm designs in the areas covered by the Spanish maritime spatial planning. Appl. Energy 381, 125165. https://doi.org/10.1016/j.apenergy.2024.125165.

Trapani, K., Redón Santafé, M., 2015. A review of floating photovoltaic installations: 2007–2013. Prog. Photovoltaics Res. Appl. 23 (4), 524–532. https://doi.org/10.1002/pip.2466.

Turney, D., Fthenakis, V., 2011. Environmental impacts from the installation and operation of large-scale solar power plants. Renew. Sustain. Energy Rev. 15 (6), 3261–3270. https://doi.org/10.1016/j.rser.2011.04.023.

Ulazia, A., Sáenz, J., Saenz-Aguirre, A., Ibarra-Berastegui, G., Carreno-Madinabeitia, S., 2023. Paradigmatic case of long-term colocated wind–wave energy index trend in Canary Islands. Energy Convers. Manag. 283, 116890. https://doi.org/10.1016/j.enconman.2023.116890.

Wei, Y., Khojasteh, D., Windt, C., Huang, L., 2025. An interdisciplinary literature review of floating solar power plants. Renew. Sustain. Energy Rev. 209, 115094. https://doi.org/10.1016/j.rser.2024.115094.

Yang, C., Cai, S., Gou, Z., 2024. Unlocking solar potential in high-latitude urban areas: a study of morphological indicators and zero energy potential of Glasgow. Sol. Energy 283, 113023. https://doi.org/10.1016/j.solener.2024.113023.